arXiv:cond-mat/0012368v1 [cond-mat.supr-con] 19 Dec 2000

Mode-locking in ac-driven vortex lattices with random pinning

Alejandro B. Kolton and Daniel Domínguez
Centro Atómico Bariloche, 8400 S. C. de Bariloche, Río Negro, Argentina

Niels Grønbech-Jensen
Department of Applied Science, University of California, Davis, CA 95616, USA
NERSC, Lawrence Berkeley National Laboratory, Berkeley, CA 94720, USA

(February 1, 2008)

We find mode-locking steps in simulated current-voltage characteristics of ac-driven vortex lattices with *random* pinning. For low frequencies there is mode-locking above a finite ac force amplitude, while for large frequencies there is mode-locking for any small ac force. This is correlated with the nature of temporal order in the different regimes in the absence of ac drive. The mode-locked state is a frozen solid pinned in the moving reference of frame, and the depinning from the step shows plastic flow and hysteresis.

PACS numbers: 74.60.Ge, 74.40.+k, 05.70.Fh

In 1971 A. T. Fiory [1] observed steps in the current-voltage (IV) characteristics of ac-driven superconducting thin films, analogous to the Shapiro steps found in Josephson junctions [2]. The steps were observed for voltages such that $2\pi\langle v\rangle/a_0 = (p/q)\Omega$, with $\langle v\rangle$ the average vortex velocity, a_0 the triangular vortex lattice period, Ω the frequency of the external ac-drive, and p, q integers. This is a particular case of mode-locking, where an internal frequency of the system (in this case $\omega_0 = \langle v\rangle 2\pi/a_0$) locks to a rational multiple of the external frequency. Several other systems with many degrees of freedom, such as charge density waves [3,4], spin density waves [5], Josephson junction arrays [6] and superconductors with periodic pinning arrays [7,8], also exhibit mode-locking behavior experimentally. Recently, Harris *et al.* [11] observed the Fiory steps in YBCO and found that they vanish when the vortex melting line is crossed. Historically, the experiment of Fiory motivated the landmark works of Schmid and Hauger [9] and Larkin and Ovchinikov [10] on the dynamics of moving vortex lattices. In [9,10] it was assumed that at large velocities vortices form a perfect triangular lattice in which the effect of random pinning could be treated perturbatively. However, it is now clear that, instead of a perfect triangular lattice, there are several other dynamical phases of driven vortices: plastic flow [12], moving smectic, transverse moving glass and moving Bragg glass [13–15]. These regimes have been observed experimentally [16] and in numerical studies [17,18]. Thus, it may be of interest to study how the Fiory steps can arise in different moving vortex phases. Moreover, a peak in the voltage noise power spectrum at the “washboard” frequency ω_0 has recently been observed experimentally in driven superconductors [19,20]. This is a signature of temporal order in the high-current steady states of moving vortices [15,21]. We here present a numerical study of mode-locking for the different regimes of vortex velocities and its relationship with temporal order.

The equation of motion of a vortex in position $\mathbf{r}_i$ is:

$$\eta\frac{d\mathbf{r}_i}{dt} = -\sum_{j\neq i}\nabla_i U_v(r_{ij}) - \sum_p \nabla_i U_p(r_{ip}) + \mathbf{F}(t), \qquad (1)$$

where $r_{ij} = |\mathbf{r}_i - \mathbf{r}_j|$ is the distance between vortices i, j, $r_{ip} = |\mathbf{r}_i - \mathbf{r}_p|$ is the distance between the vortex i and a pinning site at $\mathbf{r}_p$, $\eta = \frac{\Phi_0 H_{c2} d}{c^2\rho_n}$ is the Bardeen-Stephen friction and $\mathbf{F}(t) = \frac{d\Phi_0}{c}[\mathbf{J_{dc}} + \mathbf{J}_{ac}\cos(\Omega t)]\times\mathbf{z}$ is the driving force due to an alternating current $\mathbf{J}_{ac}\cos(\Omega t)$ superimposed to a constant current $\mathbf{J}_{dc}$. A 2D thin film superconductor of thickness d with $d \ll \lambda$, has an effective penetration depth $\Lambda = 2\lambda^2/d$. Since Λ is of the order of the sample size, the vortex-vortex interaction is considered logarithmic: $U_v(r) = -A_v \ln(r/\Lambda)$, with $A_v = \Phi_0^2/8\pi\Lambda$ [18]. The vortices interact with a random distribution of attractive pinning centers with $U_p(r) = -A_p e^{-(r/\xi)^2}$, ξ being the coherence length. Length is normalized by ξ, energy by A_v, and time by $\tau = \eta\xi^2/A_v$. We consider N_v vortices and N_p pinning centers in a rectangular box of size $L_x \times L_y$, and the normalized vortex density is $n_v = N_v\xi^2/L_xL_y = B\xi^2/\Phi_0$. Moving vortices induce a total electric field $\mathbf{E} = \frac{B}{c}\mathbf{v}\times\mathbf{z}$, with $\mathbf{v} = \frac{1}{N_v}\sum_i \mathbf{v}_i$.

We study the response of the vortex lattice to an external ac+dc force of the form $\mathbf{F} = [F_{dc} + F_{ac}\cos(\Omega t)]\mathbf{y}$ [22] at $T = 0$, solving Eq. (1) for different values of F_{ac} and Ω. The simulations are for constant vortex density $n_v = 0.04$ in a box with $L_x/L_y = \sqrt{3}/2$, and $N_v = 64, 100, 144, 196, 256, 400$ (we show results for $N_v = 256$), and we consider weak pinning strength of $A_p/A_v = 0.05$ with a density of pinning centers being $n_p = 0.08$. Periodic boundary conditions are imposed on the simulation box and the resulting long-range interaction is determined by Ref. [23]. The equations are integrated using a time step of $\Delta t = 0.001\tau$, averages are evaluated during 131072 steps after 3000 steps for equilibration (when the total energy reaches a stationary mean value).

Let us first review the behavior for $F_{ac} = 0$. There are three dynamical regimes when increasing F_{dc} above the critical depinning force, F_c, in the case $F_{ac} = 0$: plastic flow for $F_c < F_{dc} < F_p$, smectic flow for

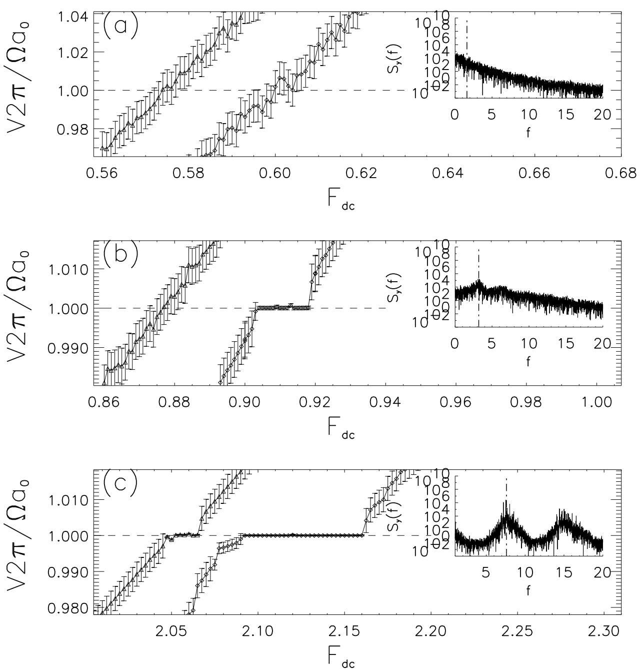

FIG. 1. Velocity-force curve around the main interference condition $V = \Omega a_0/2\pi$ for three typical drive frequencies Ω. Each case show results for two values of amplitude F_{ac} (the curves are shifted in F_{dc} for clarity). Insets show corresponding voltage power spectrum for $F_{ac} = 0$ and $V \approx V_{step}$. Vertical dashed line in the spectral density indicates the washboard frequency. (a) $\Omega = 0.5$, $F_{ac} = 0.4$ (left), $F_{ac} = 1.8$ (right). (b) $\Omega = 1$, $F_{ac} = 0.4$ (left), $F_{ac} = 3$ (right). (c) $\Omega = 2.5$, $F_{ac} = 0.75$ (left), $F_{ac} = 4$ (right).

$F_p < F_{dc} < F_t$, and a transverse solid for $F_t < F_{dc}$ (see [18]). The characteristic forces in our case are $F_c \approx 0.15$, $F_p \approx 0.6$ and $F_t \approx 1.2$. Since the nature of mode-locking is related to the existence of temporal order at the washboard frequency ω_0 we analyze the voltage noise $S_y(f) = |\frac{1}{T}\int_0^T dt(V_y(t) - V)\exp(i2\pi f t)|^2$ in each dynamical regime. In the insets of Fig. 1(a-c) we show the spectral densities corresponding to each regime and we indicate the corresponding ω_0. In the inset of Fig. 1(a) we see that there is no temporal order at the washboard frequency, and only the typical broad band noise of plastic flow is observed [12,20]. For the smectic flow regime, we see in the inset of Fig. 1(b) that there is a small and broad peak at ω_0. Only for large forces, $F > F_t$, in the transverse solid regime well developed peaks appear at the washboard frequency [20] and harmonics (see the inset of Fig. 1(c)).

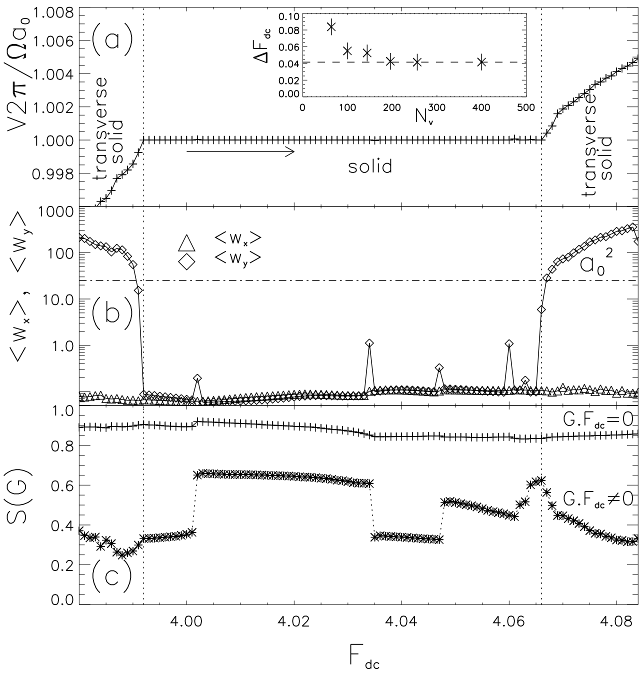

FIG. 2. (a) Velocity-force curve around the main interference step for $\Omega = 5$ and $F_{ac} = 6$. Inset shows the finite size dependence of the step width. (b) Time averaged quadratic mean displacements in the longitudinal direction $\langle w_y(t)\rangle$, ($\diamond$) points, and in the transverse direction $\langle w_x(t)\rangle$, ($\triangle$) points. The dash-dotted line indicates a_0^2. (c) Intensity of the Bragg peaks. For smectic ordering $S(G_1)$, $K_y = 0$: ($+$) points. For longitudinal ordering $S(G_{2,3})$, $K_y = 0$: ($*$) points.

We now study the response of each of these dynamical regimes with velocity $V = V(F_{dc})$ to the superimposed ac-force $F_{ac}\cos(\Omega t)$, for varying values of F_{ac} for a given Ω. We expect the main interference step ($p = q = 1$) to occur when $V = V_{step} = \Omega a/2\pi$ (*i.e.*, $\Omega = \omega_0$) if there is mode-locking. We therefore choose the values of Ω such that the expected step, $V_{step} = \Omega a/2\pi$, would correspond to velocities V belonging to a given dynamical regime of the limit $F_{ac} = 0$. Each simulation is started at $\langle v_y\rangle \approx 0.975\Omega a/2\pi$ with an ordered triangular lattice up to values such that $\langle v_y\rangle \approx 1.025\Omega a/2\pi$ by slowly increasing the dc force F_{dc} with $\Delta F_{dc} = 0.001$. For low Ω, for which we have plastic flow when $F_{ac} \to 0$, we find that there are no interference steps in a wide range of F_{ac} (shown in Fig. 1(a) for $F_{ac}/V_{step} < 1$ (left curve) and $F_{ac}/V_{step} > 1$ (right curve)). This is consistent with the observed lack of temporal order in the inset of Fig. 1(a) and indicates that very large F_{ac} are possibly needed in order to induce mode-locking. For intermediate Ω, for which we have smectic flow when $F_{ac} \to 0$, we find that there are no steps for small amplitudes, $F_{ac}/V_{step} < 1$, while there are steps for $F_{ac}/V_{step} > 1$, as shown in Fig. 1(b) in the left and right curves, respectively. This means that the small washboard peak observed in the inset of Fig. 1(b) is not large enough to induce mode-locking steps for small F_{ac}. However, this short-range temporal order can be amplified for intermediate values of F_{ac} giving place to steps in this case. For high Ω, corresponding to a transverse solid regime when $F_{ac} \to 0$ we find that there are steps both for small $F_{ac}/V_{step} < 1$ and large $F_{ac}/V_{step} > 1$ values of the ac amplitude, as we can observe in Fig. 1(c). This is in agreement with the $F_{ac} = 0$ spectral response

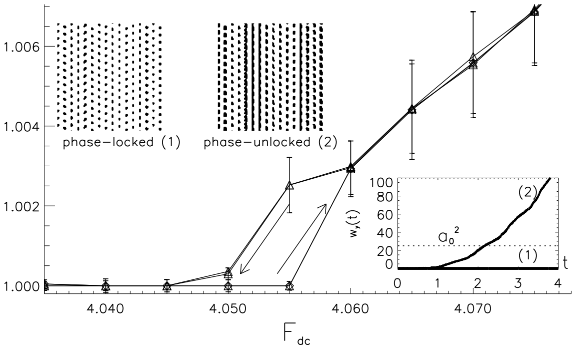

FIG. 3. Velocity-force curve around the depinning from the main step for $\Omega = 5$ and $F_{ac} = 6$. The upper left insets show typical time averaged coarse-grained density of vortices seen from a system of reference moving with velocity $v_{step} = \Omega a_0/2\pi$, for a mode-locked state $F_{dc} = 4.045$ (left) and for an unlocked state $F_{dc} = 4.085$ (right). The lower right inset shows the corresponding typical quadratic mean longitudinal displacements for both cases. Dashed line indicates a_0^2.

observed in inset of Fig. 1(c). In this case, the temporal order is robust enough for mode-locking to be produced by small values of F_{ac}.

Let us now examine in detail the dynamics and the structural order within and in the vicinity of a mode-locked step, in the transverse solid case. In Fig. 2(a) we show a typical $V - F_{dc}$ curve around the step. In the inset of Fig. 2(a) we show a finite size analysis of the step width for $N_v = 64, 100, 144, 196, 256, 400$, where the error bars are due to the observed dependence of the width in three different realizations of disorder. We observe that for $N_v > 256$ the step width tends to saturate in a size-independent value. To analyze the dynamical behavior we define the quadratic mean displacements of vortices in directions parallel $w_y(t)$ and perpendicular $w_x(t)$ to the external force, calculated from the center of mass position $(X_{cm}(t), Y_{cm}(t))$ as: $w_x(t) = \frac{1}{Nv}\sum_i[\tilde{x}_i(t) - \tilde{x}_i(0)]^2$ and $w_y(t) = \frac{1}{Nv}\sum_i[\tilde{y}_i(t) - \tilde{y}_i(0)]^2$, where $\tilde{x}_i(t) = x_i(t) - X_{cm}(t)$ y $\tilde{y}_i(t) = y_i(t) - Y_{cm}(t)$. In Fig. 2(b) we show the time average of these quantities, $\langle w_x(t)\rangle$ and $\langle w_y(t)\rangle$, as a function of F_{dc}. Outside the step we observe that the transverse mean displacement (TMD) is limited $\langle w_x(t)\rangle \ll a_0^2$, while the longitudinal mean displacement (LMD) is unbounded $\langle w_y(t)\rangle \gg a_0^2$. This corresponds to a state with only longitudinal diffusion (i.e., a transverse solid [18]). Noticeably, in the transition to the synchronization, the LMD freezes in a value, $\langle w_y(t)\rangle \ll a_0^2$, while the TMD remains practically constant. This *mode-locking longitudinal freezing* can also be observed as a dramatic decrease of the low frequency voltage noise in both directions. The mode-locked state is therefore a frozen solid. To study the translational order we calculate the structure factor as $S(\mathbf{k}) = \langle|\frac{1}{N_v}\sum_i \exp[i\mathbf{k}\cdot\mathbf{r}_i(t)]|^2\rangle$. In this regime there are smectic order peaks of magnitude $S_s = S(\mathbf{G}_1)$ with $\mathbf{G}_1 = (\pm 2\pi/a_0, 0)$ and longitudinal peaks of magnitude $S_l = (S(\mathbf{G}_2) + S(\mathbf{G}_3))/2$ with $\mathbf{G}_2 = \pm 2\pi/a_0(1/2, \sqrt{3}/2)$ and $\mathbf{G}_3 = \pm 2\pi/a_0(-1/2, \sqrt{3}/2)$. In Fig. 2(c) we plot S_s and S_l. We do not observe any important change in the transition to the mode-locked state. Inside the steps we observe jumps in S_l indicating that there are different metastable mode-locked structures. In Fig. 3 we analyze in detail the process of depinning from the step. We show a detailed view of the $V - F_{dc}$ curve in the transition from the synchronized regime. Varying F_{dc} back and forth, we observe a clear hysteresis cycle. In the lower right inset of Fig. 3 we show the evolution of $w_y(t)$ with time inside the step and outside the step. While $w_y(t) \ll a_0$ for all t inside the step, outside there is ballistic diffusion $w_y(t) \sim t^2$. To visualize the spatial structure in the transition we define a coarse-grained vortex density $\rho'_v(\mathbf{r}, t)$ seen from a system of reference moving with velocity V_{step} as follows: $\rho'_v(\mathbf{r}, t) = \frac{1}{N_v}\sum_i \delta(\mathbf{r} - \mathbf{r'}_i(t))$, where $\mathbf{r'}_i(t) = \mathbf{r}_i(t) - \mathbf{y}V_{step}t$. We take a coarse-graining scale $\Delta r < a_0$. In the upper left insets of Fig. 3 we show the temporal average $\langle\rho'_v(\mathbf{r}, t)\rangle$ of the density, inside (mode-locked) and outside (mode-unlocked) the step. This quantity shows the stationary trajectories of vortices seen from a moving frame of reference with velocity V_{step}. Inside the step we see that the vortices are localized, oscillating around their equilibrium positions in a moving lattice with velocity V_{step}. This is in agreement with the mode-locked frozen solid inferred from the result shown in Fig. 2(b), which is "pinned" in the moving reference frame with velocity V_{step}. Just above the depinning from the step we see that some vortices delocalize following straight trajectories parallel to the force around "pinned" vortices, producing coexistence of mode-locked

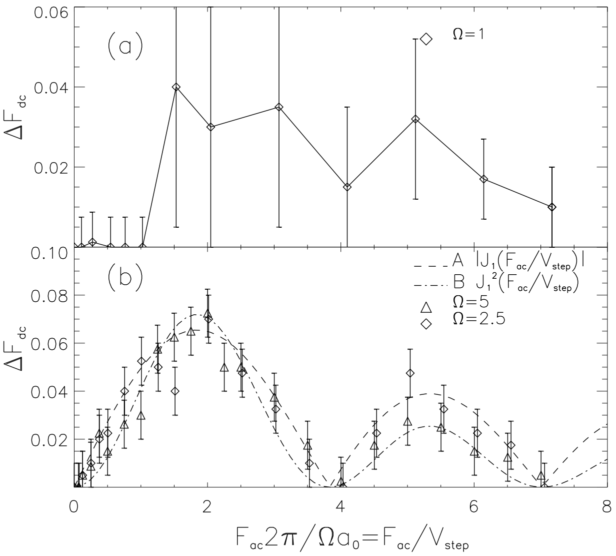

FIG. 4. Step width ΔF_{dc} vs $F_{ac}2\pi/\Omega a_0 = F_{ac}/V_{step}$. (a) $\Omega = 1$. (b) $\Omega = 5$ (△) points and $\Omega = 2.5$ (◇) points. Dashed line shows a fit to $A|J_1(F_{ac}/V_{step})|$ and the dot-dashed line a fit to $B|J_1(F_{ac}/V_{step})|^2$.

and mode-unlocked channels of flow. This could be interpreted as a one-dimensional "plastic" depinning from the step.

Mode-locking of the steps in the $V - F_{dc}$ curve can be characterized qualitatively by how the dc current range in mode-locking depends on F_{ac} and Ω, (as it was done for example in [6–8]). In Fig. 4(a-b) we show the range (width) ΔF_{dc} for the case $F_p < F_{dc} < F_t$ and $F_t < F_{dc}$ respectively. The error bars and the mean values were estimated by repeating the simulation for three different disorder realizations. In Fig. 4(a) we show ΔF_{dc} for $\Omega = 1$ vs F_{ac}, which corresponds to the smectic flow regime for $F_{ac} \to 0$. We see that there is mode-locking above a finite critical value $F_{ac}/V_{step} \approx 1$ (see Fig. 1(b)). For larger amplitudes we were not able to obtain a systematic dependence on amplitude because the step widths depend strongly on the disorder realization in this case. In Fig. 4(b) we show ΔF_{dc} for two frequencies $\Omega = 2.5, 5$ vs F_{ac}, which correspond to the transverse solid in the $F_{ac} = 0$ limit. We can collapse (approximately) both curves into a single curve if we plot ΔF_{dc} vs F_{ac}/V_{step}. A dependence, $\Delta F_{dc} \sim (1/C_{66})|J_1(F_{ac}/V_{step})|^2$, was found by Schmid and Hauger [9] (and also found in other elastic models) where $V_{step} = a_0\Omega/2\pi$ and C_{66} is the shear modulus. This result was obtained using a perturbative approach in an elastic model for the vortex lattice. Strikingly, our results seem to follow more closely a dependence of the form $\Delta F_{dc} \approx A|J_1(F_{ac}/V_{step})|$ with A being a constant. This dependence is the same found for the one-dimensional problem of an overdamped single Josephson junction or a particle moving in a periodic potential. In our case, a linear dependence of the mode-locking intensity with F_{ac} would be a consequence of the existence of temporal order in the $F_{ac} = 0$ limit. This was not taken into account in the perturbative calculation of Schmid and Hauger where mode-locking arises as a second order effect.

In conclusion, it is possible to have mode-locking in driven vortices with *random* pinning for high enough frequencies, in agreement with the experiments of Fiory [1] and Harris *et al* [11]. The mode-locked state can be viewed as a frozen solid pinned in the moving frame of reference, and the depinning from mode-locking is plastic and hysteretic. Also, the response to an ac drive for different frequencies can be an interesting experimental probe of the dynamical regimes of driven vortices.

We acknowledge discussions with L. Balents, P. S. Cornaglia, M. F. Laguna, V. I. Marconi. This work has been supported by CONICET, Fundación Antorchas and ANPCYT (Argentina) and by the Director, Office of Advanced Scientific Computing Research, Division of Mathematical, Information and Computational Sciences of the U.S. Department of Energy under contract number DE-AC03-76SF00098.

---

[1] A. T. Fiory, Phys. Rev. Lett. **27**, 501 (1971); Phys. Rev. B **7**, 1881 (1973); Phys. Rev. B **8**, 5039 (1973).
[2] S. Shapiro, Phys. Rev. Lett. **11**, 80 (1963).
[3] G. Gruner, Rev. Mod. Phys **60**, 1129 (1988); S. Bhattacharya *et al.*, Phys. Rev. Lett. **59**, 1849 (1987); M. H. Higgins, A. Alan Middleton, and S. Bhattacharya, *ibid.* **70**, 3784 (1993).
[4] L. Sneddon, M. C. Cross and D. S. Fisher, Phys. Rev. Lett. **49**, 292 (1982); S. N. Coppersmith and P. B. Littlewood, *ibid.* **57**, 1927 (1986); A. A. Middleton *et al.*, *ibid.* **68**, 1586 (1992).
[5] E. Barthel *et al.*, Phys. Rev. Lett. **71**, 2825 (1993).
[6] S. Benz *et al.*, Phys. Rev. Lett. **64**, 693 (1990).
[7] P. Martinoli *et al.*, Solid State Commun, **17**, 207 (1975); L. Van. Look *et al.*, Phys. Rev. B **60**, R6998 (1999).
[8] C. Reichhardt *et al.*, Phys. Rev. B **61**, R11914 (2000).
[9] A. Schmid and W. Hauger, J. Low. Temp. Phys. **11**, 667 (1973).
[10] A. I. Larkin and Yu. N. Ovchinikov, Zh. Eksp. Teor. Fiz **65**, 1704 (1973) [Sov. Phys. JETP **38**, 854 (1974)].
[11] J. M. Harris *et al.*, Phys. Rev. Lett. **74**, 3684 (1994).
[12] H. J. Jensen *et al.*, Phys. Rev. Lett. **60**, 1676 (1988); A.-C. Shi and A. J. Berlinsky, Phys. Rev. Lett. **67**, 1926 (1991).
[13] A. E. Koshelev and V. M. Vinokur, Phys. Rev. Lett. **73**, 3580 (1994); S. Scheidl and V. M. Vinokur, *ibid.* **57**, 13800 (1998).
[14] T. Giamarchi and P. Le Doussal, Phys. Rev. Lett. **76**, 3408 (1996); P. Le Doussal and T. Giamarchi, Phys. Rev. B **57**, 11356 (1998).
[15] L. Balents, M. C. Marchetti and L. Radzihovsky, *ibid.* **57**, 7705 (1998);
[16] S. Bhattacharya and M. J. Higgins, Phys. Rev. Lett. **70**, 2617 (1993); U. Yaron *et al.*, Nature (London) **376**, 743 (1995); M. C. Hellerqvist *et al.*, Phys. Rev. Lett. **76**, 4022 (1996); F. Pardo *et al*, *ibid.* **396**, 348 (1998).
[17] K. Moon, R. T. Scalettar and G. Zimányi, Phys. Rev. Lett. **77**, 2778 (1996); S. Ryu *et al.*, *ibid.* **77**, 5114 (1996); N. Grønbech-Jensen, A. R. Bishop and D. Domínguez, *ibid.* **76**, 2985 (1996); C. Reichhardt *et al.*, *ibid.* **78**, 2648 (1997); D. Domínguez, N. Grønbech-Jensen and A.R. Bishop, *ibid.* **78**, 2644 (1997); C. J. Olson, C. Reichhardt and F. Nori, *ibid.* **81**, 3757 (1998); D. Domínguez, *ibid.* **82**, 181 (1999).
[18] A. B. Kolton, D. Domínguez and N. Grønbech-Jensen, Phys. Rev. Lett. **83**, 3061 (1999); A. B. Kolton *et al.*, Phys. Rev. B **62**, R14657 (2000).
[19] A. M. Troyanovski, J. Aarts, and P. H. Kes, Nature **399**, 665 (1999).
[20] Y. Togawa *et al.*, Phys. Rev. Lett. **85**, 3716 (2000).
[21] L. Balents and M. P. A. Fisher, Phys. Rev. Lett. **75**, 4270 (1995).
[22] The case of $\mathbf{F}_{ac} \perp \mathbf{F}_{dc}$ will be studied separately.
[23] N. Grønbech-Jensen, Int. J. Mod. Phys. C **7**, 873 (1996); Comp. Phys. Comm. **119**, 115 (1999).